Interplay between phosphoinositides and actin cytoskeleton in the regulation of immunity related responses in Arabidopsis thaliana seedlings

Tetiana Kalachova, Romana Pospichalova, Petr Marsik, Pavel Kloucek, Olga Valentová, Eric Ruelland, Hana Leontovyčová, Oksana Iakovenko, Petr Maršík, Pavel Klouček, et al.

Interplay between phosphoinositides and actin cytoskeleton in the regulation of immunity related responses in *Arabidopsis thaliana* seedlings

Tetiana KALACHOVA[1+]*, Hana LEONTOVYČOVÁ[1,2,3+], Oksana IAKOVENKO[1,2,4+], Romana POSPÍCHALOVÁ[1], Petr MARŠÍK[5], Pavel KLOUČEK[5], Martin JANDA[1,2,6], Olga VALENTOVÁ[2], Daniela KOCOURKOVÁ[1], Jan MARTINEC[1], Lenka BURKETOVÁ[1], Eric RUELLAND[6,7]

[1]Institute of Experimental Botany, The Czech Academy of Sciences, Rozvojová 263, Prague 160 000, CZECH REPUBLIC

[2]University of Chemistry and Technology Prague, Department of Biochemistry and Microbiology, Prague 166 28, CZECH REPUBLIC

[3]Department of Biochemistry, Faculty of Science, Charles university, Hlavova 8, 128 43, CZECH REPUBLIC

[4]V.P. Kukhar Institute of Bioorganic Chemistry and Petrochemistry, National Academy of Sciences of Ukraine, 1 Murmanska street, 02094 Kyiv, UKRAINE

[5]Department of Food Quality and Safety, Faculty of Agrobiology, Food and Natural Resources, Czech University of Life Sciences Prague, Kamýcká 129, 165 00 Prague, CZECH REPUBLIC

[6]Ludwig-Maximilians-University of Munich (LMU), Faculty of Biology, Biocenter, Department Genetics, Grosshaderner Str. 2-4, D-82152 Martinsried, GERMANY

[7]CNRS, Institut d'Ecologie et des Sciences de l'Environnement de Paris, UMR 7618, Créteil, FRANCE

[8]Université Paris-Est, UPEC, Institut d'Ecologie et des Sciences de l'Environnement de Paris, Créteil, FRANCE

[+] equally contributed

* corresponding author; kalachova@ueb.cas.cz

Runing title: Actin filaments, callose and phosphatidylinositol-4-kinase mutants

Keywords: Actin, Latrunculin B, Salicylic acid, Callose, Phosphatidylinositol-4-kinase

ABSTRACT

Actin cytoskeleton is indispensable for plant cell integrity. Besides, increasing evidences illustrate its crucial role in plant responses to environment, including defence against pathogens. Recently, we have demonstrated that pre-treatment with actin disrupting drugs latrunculin B (latB) and cytochalasin E can enhance plant resistance against bacterial and fungal pathogens via activation of salicylic acid (SA) pathway. Here, we show that actin depolymerization in *Arabidopsis thaliana* seedlings not only triggers SA biosynthesis by ICS1, but also induces callose deposition via callose synthase PMR4. This effect is SA-independent since still present in mutants that do not accumulate SA. LatB also triggers the expression of several defence related genes. We could distinguish genes, induced in a SA-dependent manner (*PR1*, *WRKY38*, *ICS1*) and those that are SA-independent (*PR2*, *PAD4*, *BAP1*). As actin cytoskeleton is tightly connected with membrane trafficking, we assayed the effect of latB on mutant plants invalidated in phosphatidylinositol 4-kinase beta1 and beta2 (PI4Kβ1β2). Deficiency in PI4Kβ1β2 enhanced latB-triggered actin filaments depolymerisation. Yet, it did not lead to a stronger callose deposition or SA biosynthesis in response to latB. Surprisingly, introduction of *NahG* construct or *pad4* mutation in *pi4kß1ß2* background had much lower effect on SA induction and SA-dependent gene expression changes than it has in wild type. We can thus conclude that actin disruption itself triggers immune-like responses: there is an induction of SA *via* PAD4 coupled to ICS1; it leads to the induction of *PR1* and *WRKY38,* and this requires a functional PI4Kβ1β2 to be properly regulated. However, an alternative, SA-independent, pathway also exists that leads to the enhanced expression of *PR2* and to callose accumulation.

INTRODUCTION

Plants are always confronted to changes in their environment. This can concern physical parameters such as light intensity and/or quality, temperature or water availability, or interactions with other organisms, including bacteria or fungi. Some of the interactions can lead to diseases. Nowadays, plant responses to the environmental challenges, either abiotic or biotic, are an object of an intense research. A novel aspect of such a research is the investigation of the roles of processes that were so far mainly (or uniquely) considered as important for the cell structure. Such a process is the dynamics of cytoskeleton. Cytoskeleton is comprised of microfilaments and microtubules. Actin filaments (F-actin) are highly dynamic structures formed from monomers (G-actin) (Drobak et al, 2004). Even in basal conditions, filaments constantly grow at one end and depolymerize at the opposite one (Li et al, 2017). The filaments are indispensable for cell shaping, growth and polarity (Andreeva et al, 2010), cytokinesis (Brill et al, 2000), but also for intracellular trafficking of vesicles (Geitmann & Nebenführ, 2015). Yet, the direct mechanisms regulating actin dynamics in regards to vesicle trafficking are still waiting to be revealed. A particular role has been proposed for phospholipids, especially phosphoinositides (Ebine & Ueda, 2015). Phosphoinositides are phosphorylated forms of phosphatidylinositol (PI). From the position and number of the phosphate groups on the inositol ring, we can distinguish PI-3-phosphate (PI3P), PI-4-phosphate (PI4P) and PI-4,5-bisphosphate (PIP_2). Phosphoinositides play a key role in vesicle trafficking (Delage et al, 2013) and also interact with cytoskeleton: for instance, F-actin capping protein interaction with actin monomers is regulated by PIP_2 (Pleskot et al, 2012). This makes phosphoinositides potential central players in the regulation of cytoskeleton dynamics versus vesicle trafficking. Phosphatidylinositol-4 kinases (PI4Ks) are the first enzymes committing PI into phosphoinositides phosphorylated at position 4 of inositol. The study of these enzymes and of their corresponding mutants can be useful to investigate the regulation of the vesicle trafficking together with cytoskeleton dynamics. In *Arabidopsis thaliana*, the isoforms AtPI4Kβ1 and AtPI4Kβ2 appear to be located in the endomembrane system (Antignani et al, 2015; Kang et al, 2011). They participate in cytokinesis in *A.thaliana* roots by targeting actin filaments to the cell plate (Lin et al, 2019).

Regarding cytoskeleton and the responses to pathogens, it must be noted that soon after contact between a plant cell and a pathogen, actin filaments get rapidly reordered to support transport of the stress-related compounds. For instance, in the case of fungal infection, actin is

needed for the transport of antimicrobial compounds and callose to the penetration site (Hardham, 2007). This results in forming cell wall appositions that arrest pathogen growth at the invaded cell (Sassmann et al, 2018). This is part of plant immunity response. In case of bacterial infection, the reaction at the level of cytoskeleton is more diffuse along the leaf tissue but an increase of actin filament density and bundling can nevertheless be measured (Lu & Day, 2017). Various components of pathogen cells can trigger actin polymerization in plants. The most described are the so-called microbe associated molecular patterns (MAMPs), like flagellin flg22, elf18, chitin, oligogalacturonides (Li et al, 2017), or secreted effectors (e.g. HopG1 of *Pseudomonas syringae*, (Shimono et al, 2016). Those compounds not only affect cytoskeleton, but induce other immune responses, especially reactive oxygen species formation, defence genes expression, biosynthesis of salicylic acid (SA) (Bigeard et al, 2015).

A well described response to pathogens is callose accumulation (Schneider et al, 2016). Callose is a polysaccharide, β-1,3-glucan, synthetized in the apoplast and involved in various processes in plants including cytokinesis (Chen et al, 2009; Thiele et al, 2009), pollen development (Záveská Drábková & Honys, 2017), cell-to-cell communication through plasmodesmata (Cui & Lee, 2016), and various stress responses. Arabidopsis genome encodes twelve callose synthases, each of a specific function (Chen & Kim, 2009). Callose synthase 12 (also known as GLUCAN-SYNTHASE LIKE 5, GSL5, of POWDERY MILDEW RESISTANT 4, PMR4) is the one responsive to wounding and pathogen responses (Ellinger et al, 2014; Keppler et al, 2018). Callose biosynthesis in the apoplast and its accumulation highly depend on the transport of the substrates outside of the cells. Notably, distinct signaling pathways may result in callose formation. For instance, wounding-induced and MAMP-triggered callose might represent different branches of responses going through PMR4 (Keppler et al, 2018). We therefore wanted to investigate the influence of actin depolymerization on callose accumulation. An elegant way to investigate the role of cytoskeleton is the use of drugs that alter cytoskeletal dynamics. Latrunculin B (latB) is such a drug. It originates from a Red Sea sponge *Latrunculia magnificans.* LatB reversely binds actin monomers preventing their polymerization (Morton et al, 2000). It is often used in plant biology to assess the role of actin in endo- and exocytosis (Moscatelli et al, 2012), pollen tube elongation (Gibbon et al, 1999) and growth (Baluška et al, 2001). Concerning the response to pathogens, it has been shown that when applied simultaneously with pathogens, latB negatively affects plant resistance to them (Henty-Ridilla et al, 2013). However, latB is able to activate SA-

associated gene expression in *Arabidopsis thaliana* (Matoušková et al, 2014). In *Brassica napus* and *Nicotiana benthamiana*, the pre-treatment of plant leaves with low concentrations of latB - increased SA levels in tissues, activated defence gene expression and was sufficient to increase resistance to further infection. Similar results were obtained with another actin disrupting drug, cytochalasin E (Leontovyčova et al, 2019).

We firstly show that actin disruption by latB triggers callose accumulation in *A. thaliana* seedlings through the callose synthase PMR4. Using mutants altered in SA signaling (*pad4*), biosynthesis (*sid2*) and accumulation (*NahG*), we demonstrate that this callose deposition is SA-independent. Furthermore, we found that latB effect on gene expression does not correspond to a general transcriptome deregulation, but that specific pathways related to the response to pathogens are the ones triggered by latB. Amongst the gene responses, we were also able to reveal SA-dependent and SA-independent effects of latB. Interestingly, we show that deficiency in PI4Kβ1β2 enhanced the susceptibility of actin filaments to latB while latB does not appear to impact phosphoinositides levels on plasma membrane. To study the role of PI4Kβ1β2 in SA-independent responses to actin disruption, we have introduced *NahG* construct as well as *sid2* and *pad4* mutations into *pi4kβ1β2* background. Surprisingly, the latB treatment still strongly induced SA in *pad4pi4kβ1β2* and *NahGpi4kβ1β2* triple mutants, while SA accumulation was prevented in *pad4* and *NahG* mutant plants. To conclude, here we characterize the immunity-like responses to latB, showing that actin depolymerisation acts through both SA-dependent and SA-independent pathways. Moreover, we reveal the existence of an unexpected cross-talk between actin filaments and phosphoinositides in the regulation of those defence-related responses.

Materials and methods

Plant material

The following *Arabidopsis thaliana* genotypes were used: Columbia-0 (WT); *NahG* (Delaney et al, 1994); *NahGpi4kβ1β2 (Šašek et al, 2014); pad4.1* (NASC stock N3806)*; pad4pi4kβ1β2* (this study); *sid2, pi4kß1ß2, sid2pi4kß1ß2 (Kalachova et al, 2019)*; *pmr4*; pUBQ::PMR4-GFP in WT background; pUBQ::PMR4-GFP in *pmr4* background (Kulich et al, 2018); Lifeact-GFP (Cvrčková & Oulehlová, 2017); pUBQ::mCitrine-2xFAPP1 (Simon et al, 2014).

Plant cultivation and treatment

Seedlings were grown in MS medium, containing 4.41 g Murashige and Skoog medium including vitamins (Duchefa, Netherlands) and 5 g sucrose per litre, pH adjusted to 5.7 using 1M KOH. Surface-sterilized seeds were sown in 24-well plates, 4-5 seeds per well containing 400 µL of medium and cultivated for 10 days before treatment under a short-day photoperiod (10 h/14 h light/dark regime) at 100-130 µE m^{-2} s^{-1} and 22°C. On the 7th day, 200 µL of fresh medium was added to the wells.

Latrunculin B (latB, Sigma-Aldrich, USA) was dissolved in DMSO at 2 mM stock solution. The seedlings were treated 24 h with 200 nM latB and 0.01% DMSO as mock control prior to sampling.

Gene expression analysis

The whole seedlings (approximatively 300 µg fresh weight) from three wells were immediately frozen in liquid nitrogen. The tissue was homogenized in plastic Eppendorf tubes with 1 g of 1.3 mm silica beads using a FastPrep-24 instrument (MP Biomedicals, USA). Total RNA was isolated using Spectrum Plant Total RNA kit (Sigma-Aldrich, USA) and treated with a DNA-free kit (Ambion, USA). Subsequently, 1 µg of RNA was converted into cDNA with M-MLV RNase H^- Point Mutant reverse transcriptase (Promega Corp., USA) and an anchored oligo dT21 primer (Metabion, Germany). Gene expression was quantified by qPCR using a LightCycler 480 SYBR Green I Master kit and LightCycler 480 (Roche, Switzerland). The PCR conditions were 95 °C for 10 min followed by 45 cycles of 95 °C for 10 s, 55 °C for 20 s, and 72 °C for 20 s. Melting curve analysis was then conducted. Relative expression was normalized to the housekeeping gene *AtTIP41*. A list of the analysed genes and primers is available in Supplemental table ST1.

Trypan blue and anilin blue staining

Seedlings were immersed into the staining solution (10 mL lactic acid (85%, w:w), 10 mL phenol, 10 mL glycerol, 10 mL distilled H_2O, 40 mg trypan blue) for 2 min (Fernández-Bautista et al, 2016). Seedlings were then washed twice in ethanol:glacial acetic acid (1:3, v:v) until leaves were fully decoloured. Seedlings were rehydrated by incubating in ethanol solutions of decreasing concentrations (70%, 50%, 30%, v:v) for at least 30 min each. They were then stained in 0.01 % aniline blue in 150 mM K_2HPO_4, pH 9.5 for 4h and kept in water for the microscopy observation.

Callose imaging and quantification

Callose deposition was observed by fluorescence microscope using a Zeiss AxioImager ApoTome2 (objective 5x). Callose accumulation was calculated using FIJI software (https://fiji.sc/) (Schindelin et al, 2012) as the percent occupancy of aniline blue signal (spots) per region of interest (ROI). One round-shaped ROI (d=1500 µm) was taken from one cotyledon, at least 18 independent cotyledons were analysed per variant.

Confocal microscopy

For *in vivo* microscopy, a Zeiss LSM 880 inverted confocal laser scanning microscope (Carl Zeiss AG, Germany) was used with either a 40× C-Apochromat objective (NA = 1.2 W) or a 20x Plan-Apochromat objective (NA = 0.8). Fluorescence associated with actin filaments (LifeAct-GFP) or phosphoinositides (mCitrine-2xFAPP1) was acquired at excitation 488 nm emission 490–540 nm for GFP and excitation 516nm emission 520-552 nm for mCitrine. Images were acquired at in z-stacks 20µm thickness). Actin filaments density analysis was calculated by Fiji software as the percent occupancy of GFP/mCitrine signal in each Maximum intensity projection. For Lifeact-GFP, image threshold was set to include all actin filaments and area fraction was measured. For each variant, fluorescent intensity of at least 30 ROI (50x50µm) from 10-14 leaves was analysed.

Salicylic acid measurement

All seedlings from 3 wells were sampled as 1 sample, frozen in nitrogen and stored at -80°C until the analysis. Samples were homogenized in tubes with 1.3 mm silica beads using a FastPrep-24 instrument (MP Biomedicals, CA, United States) with 2 x 500 µl of extraction reagent methanol/water/formic acid (15:4:1, v:v:v) supplemented with stable isotope-labelled 13C-SA internal standards, each at 100 ng per sample, to check the recovery during the purification and to validate the quantification. Extract was subjected to solid phase extraction using Oasis MCX cartridges (Waters Co., Milford, MA, United States) and eluted with methanol. The eluate was evaporated to dryness and dissolved in 30 µl of 15% acetonitrile/water (v/v) immediately before the analysis. immediately before the analysis. Quantification was performed on an Ultimate 3000

high-performance liquid chromatograph (UHPLC, Dionex; Thermo Fisher Scientific, Waltham , MA, United States) coupled to IMPACT II Q-TOF ultra-high resolution and high mass accuracy mass spectrometer (HRAM-MS; Bruker Daltonik, Bremen, Germany). Separation was carried out using column Acclaim RSLC 120 C18 (2.2 μm, 2.1x100 mm; Thermo Fisher Scientific, Waltham, MA, United States) tempered at 30°C and mobile phase consisting of 0.1% formic acid (A) and methanol (B) by gradient elution. The gradient started at 1%B and going to 39 % B in 3min, 60 % B in 7 min, 100 % B in 8 min, followed by 3 min of washing by 100% B and 5 min equilibration at initial conditions (1%B). Flow rate was changing during separation from 200 μl/min to 300 μl/min in 7 min and then kept at this rate to 16 min. Injection volume was 5 μL. The full-scan data were recorded in negative electrospray ionization (ESI) mode and processed using Data Analysis 4.3 and TASQ 1.4 software (both Bruker Daltonik, Bremen, Germany). SA and labelled internal standard ($^{13}C_6$-SA) were monitored as ions of their deprotonated molecules [M-H]- (137.0239 m/z and 143.0440 m/z, respectively). SA content was expressed in ng/g fresh weight (FW).

RESULTS

Latrunculin B induces callose *via* PMR4 callose synthase

Ten-day-old *A. thaliana* seedlings were treated for 24 h with 200 nM latB. As expected, latB treatment caused actin disruption, measured as the decrease of filament abundancy (fig.S1). The concentration used for the drug did not lead to cell death (fig.S1). More unexpectedly, the treatment also caused callose accumulation (measured as the area occupied with callose spots) (fig.1A,B).

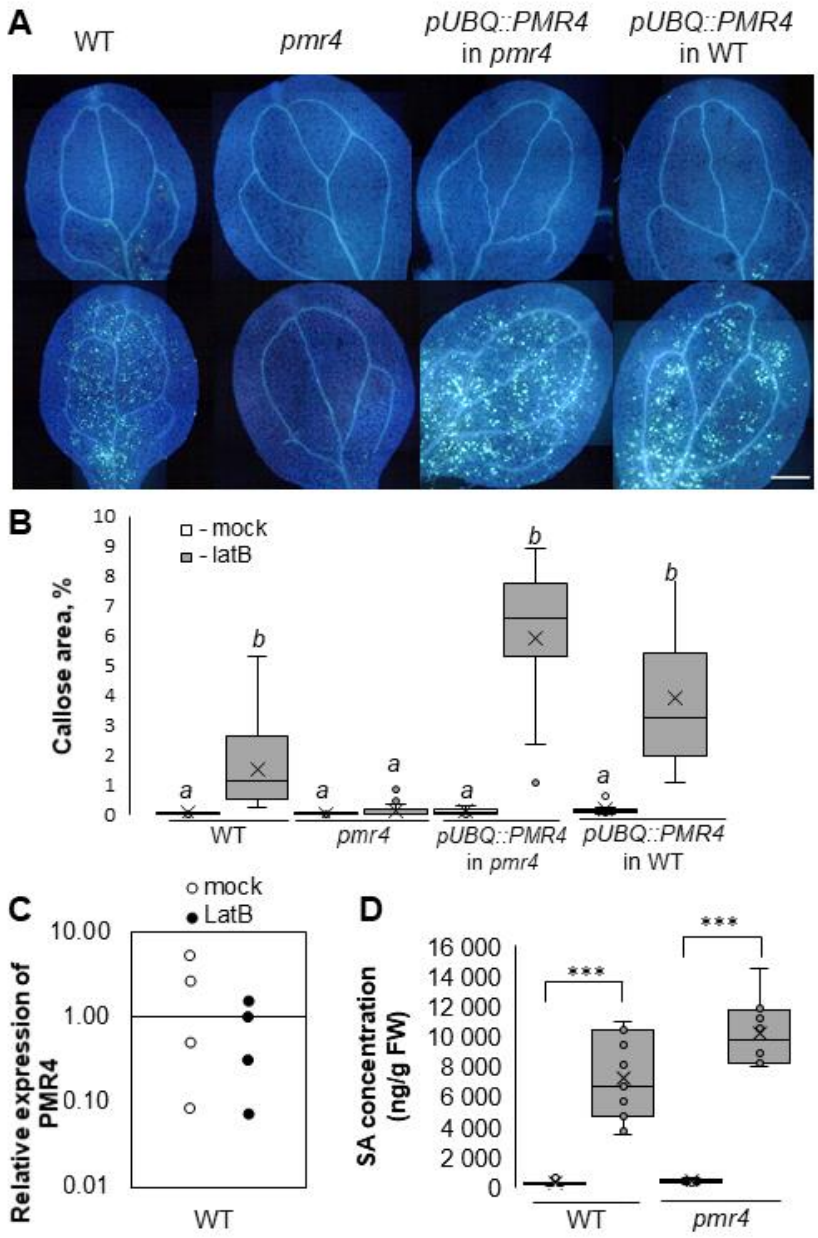

Figure 1. Latrunculin B (latB) induces PMR4-dependent callose accumulation. Ten days old *A. thaliana* seedlings were treated for 24h with 0.05% DMSO (mock) of 200 nM latB. A. Representative images of aniline blue stained cotyledons of WT, *pmr4*, pUBQ::PMR4-GFP in *pmr4*, and pUBQ::PMR4-GFP in WT, epifluorescent microscopy, scale bar = 500µm. B. Quantification of the relative area occupied with callose particles, n=18. Values for the mock-treated plants are presented in white boxes, latB treated - in dark grey boxes. In the plots, central line represents the median occupancy, cross represents the mean, bottom and top edges of the box are 25 and 75% of distribution and the ends of whiskers are set at 1.5 times the interquartile range. Values outside this range are shown as outliers. Different letters indicate variants that are significantly different, one-way ANOVA with Tukey-HSD test, $p<0.05$. C. Relative expression of *PMR4*. Relative expression of *PMR4* in WT plants. Values were normalized for the untreated WT.

TIP41 was used as the reference gene. D. Salicylic acid content. *** - variants are significantly different, two-tailed *t*-test, $p<0.001$, n=8.

Among twelve known callose synthases in *A. thaliana,* PMR4 was shown to be a major one involved to biotic stress responses (Nishimura et al., 2003; Kulich et al., 2018). We therefore tested its contribution to latB-triggered callose. In the *pmr4* mutant seedlings, the callose level detected after latB treatment was nearly equal to that in mock-treated control. When a pUBQ::PMR4-GFP construct was expressed in WT or *pmr4* backgrounds, basal callose level in cotyledons remained low. Yet, when latB was added, callose accumulation was restored (Fig. 1B). Besides, such an induction did not rely on transcriptional changes, as soon as the expression of *PMR4* was not affected (Fig. 1C).

Latrunculin B effects on callose accumulation is SA-independent

The fact that latB treatment causes callose accumulation through PMR4 strongly suggests that other defence-related responses should be studied. We therefore decided to study the role of SA content and signaling pathway in the observed callose deposition. To do so, we first measured SA levels in seedlings after latB treatment. A 20-fold increase of SA was observed in WT seedlings. Notably, *pmr4* plants behaved similarly to WT, suggesting callose to be either downstream, either independent on SA (fig. 1D, Supplementary table ST3). To address this, we analyzed SA induction and callose deposition in plants with altered SA pathway: *NahG* mutant plants, expressing the bacterial salicylate hydroxylase that degrades SA to inactive catechol and therefore unable to accumulate SA; *sid2* plants, deficient in ISOCHORISMATE SYNTHASE 1 (ICS1); and *pad4* plants, with a mutation in PHYTOALEXIN DEFICIENT 4 (PAD4) (fig.2, Supplementary table ST3). PAD4 protein has been shown to regulate the synthesis of SA *via* the ICS1 pathway (Cui et al, 2017). As expected, both *NahG* and *pad4* plants had lower basal content of SA, and smaller (approx. 5-fold) increase in SA after latB comparing to WT. *sid2* plants showed no increase in SA, pointing out that the detected SA was produced by ICS1. On the contrary, callose production was not affected any of the studied mutants, confirming SA-independent nature of the process (fig. 2, B,C).

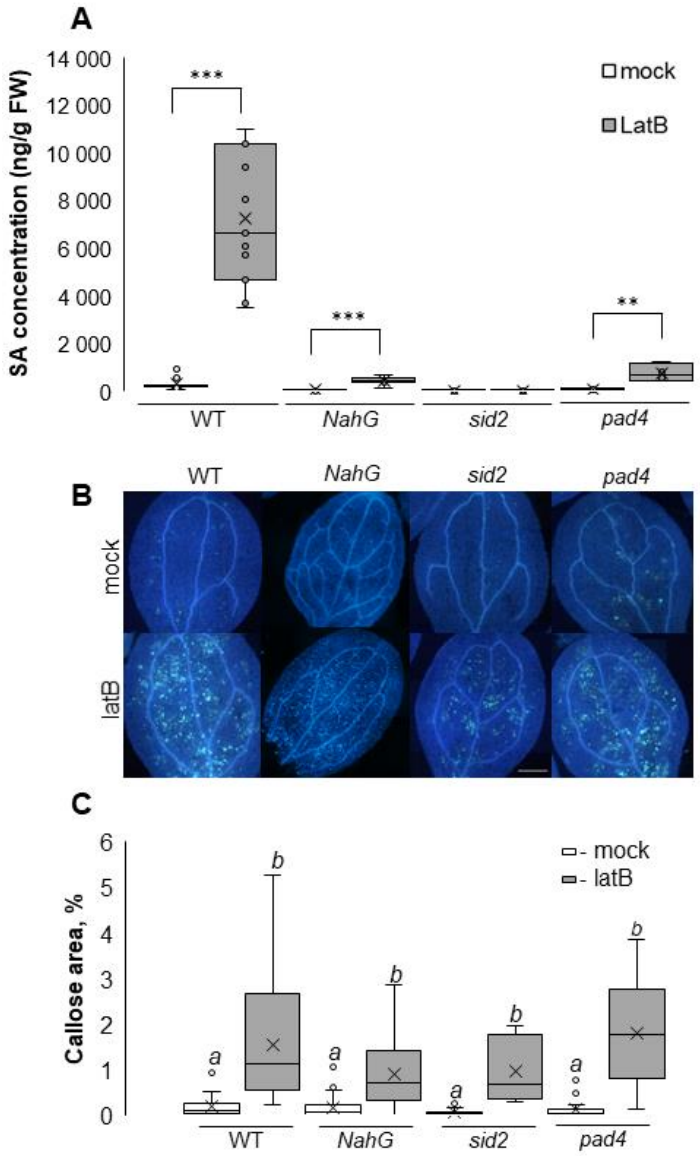

Figure 2. SA-independent induction of callose accumulation by latB treatment. Ten-day-old seedlings of WT, *NahG, sid2* and *pad4* were treated by 200 nM latB or 0.01 % DMSO as the control. Seedlings were harvested 24 hr after the treatment A. SA content. *** - samples are different, p<0.001, two-tailed *t*-test. B. Representative images of aniline blue stained cotyledons, scale bar 500 µm. C. Relative area of callose particles. Central line of the boxplot represents the median occupancy, cross represents the mean, bottom and top edges of the box are 25 and 75% of distribution and the ends of whiskers are set at 1.5 times the interquartile range. Values outside this range are shown as outliers. Different letters indicate variants that are significantly different, one-way ANOVA with Tukey-HSD test, $p<0.05$. At least 30 independent cotyledons were analysed for each variant.

Latrunculin B affects gene expression in both SA-dependent and -independent manner

We had already shown that latB could induce the expression of some genes related to plant defence (Leontovyčova et al, 2019; Matoušková et al, 2014). Here we studied whether intracellular level of SA or an intact SA-signaling pathway is needed for latB to trigger gene expression changes (figure 3, Supplementary figure S2, Supplementary table ST2). To do so, we analysed the expression of several defence marker genes in *NahG* and *pad4* mutants. Eleven-day-old *in vitro* grown plants (whole seedlings) of WT and mutant genotypes were harvested for gene expression studies 24 hpt by 200nM latB. Concerning the gene response in WT plants, we show here that the defence-associated *PR1*, *PR2*, *WRKY38*, *ICS1* and *PAD4* were induced by latB (Figure 3). We also detected an activation of the wounding marker *BAP1*, even though no cell death was yet detected by trypan blue staining (Supplemental figure S1). On the contrary, no significant changes were observed in the expression of SA biosynthetic genes other than *ICS1* (*ICS2, PAL1, PAL2, PAL3*). To be noted, ICS2 expression seems to be very dependent on the growth conditions, as we previously detected its induction after latB treatment (Leontovyčova et al, 2019). In addition, neither jasmonate biosynthesis marker genes (*LOX2, AOS1*), nor jasmonate responsive genes (*VSP2* and *PDF1.2*), nor ethylene marker gene (*ERF1*) were significantly affected by the treatment (Supplemental figure S2, Supplemental Table ST2).

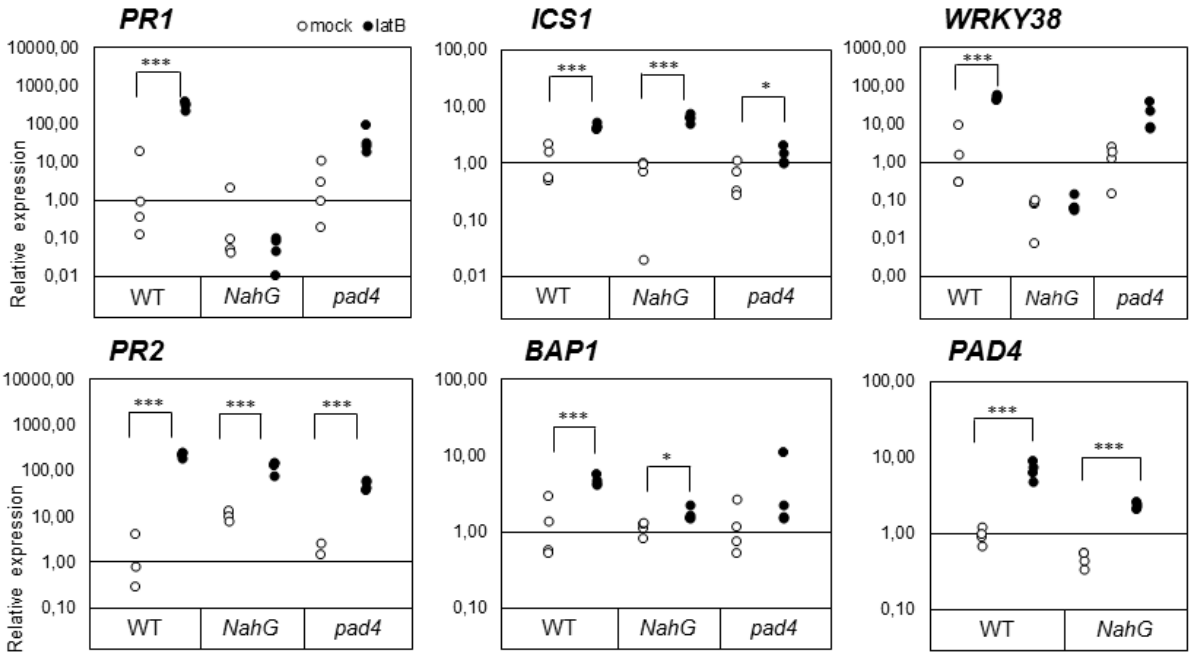

Figure 3. SA-independent expression of defence-related genes by latB treatment. Ten-day-old seedlings of WT, *NahG* and *pad4* were treated by 200 nM latB or 0.01 % DMSO as the control. Seedlings were harvested 24 hr after the treatment. Data from the representative experiment are shown. Values were normalized for mock treated WT, note that data are plotted at the $\log_{10}$ scale. Asterisks indicate values, different from respective controls for each genotype, * - p<0,05; *** - p<0.001, two-tailed Student *t*-test). Reference gene *TIP41*.

However, we detected that *PR1* and *WRKY38* inductions by latB were abolished in *NahG* and *pad4* mutants, strongly suggesting these inductions rely on a SA-dependent pathway (fig.3). This also involves that SA is accumulated in response to latB (Fig.2 A). On the contrary, the expression of *PR2* in response to latB appears not to be dependent on SA since it was still present in *NahG* and *pad4* mutants. Similarly, the expression of the *PAD4* by latB was still present in *NahG* plants: it does not rely on SA accumulation. The expression of *ICS1* in response to latB does not appear to be controlled by SA level in the tissues, as seen in *NahG* mutant. Yet, PAD4 protein regulates *ICS1* expression, at least partly. As for the induction of the expression of *BAP1* by latB, it was diminished in *NahG* and *pad4* mutants (though still present), and so can be considered as partly SA-dependent.

We can thus conclude that latB induces several defence-like responses: there is an induction of SA; it leads to the induction of *PR1* and *WRKY38*. However, an alternative, SA-independent, pathway also exists. It controls the expression of *PR2*, *ICS1*, *PAD4* and callose accumulation in response to latB.

Effects of latB on cytoskeleton are enhanced in pi4kß1ß2 double mutant

Phosphoinositides, that are the phosphorylated forms of phosphatidylinositol (PI), are involved in vesicular trafficking. This process requires correct actin cytoskeleton organization (Pleskot et al, 2014). There is therefore a link between actin cytoskeleton and phosphoinositides. We wanted to investigate whether the effect of latB could be impacted by a modification in phosphoinositide metabolism. To do so, we used the *pi4kß1ß2* double mutant. This mutant is invalidated in the two beta isoforms of phosphatidylinositol-4-kinases. This double mutant was shown to have impaired vesicle trafficking, dwarf phenotype and increased SA level (Kang et al, 2011; Šašek et al, 2014).

We firstly introduced LifeAct-GFP construct into *pi4kß1ß2* background by crossing. Four independent lines were tested. No major defects in actin filaments organization in epidermal cells were observed while compared to WT (fig.4). After 24h of latB treatment, the density of the

filaments in *pi4kß1ß2* plants was 20-times lower than that in non-treated double mutant, while in the WT background this decrease was 5-fold. Consequently, in *pi4kß1ß2* plants the actin filaments were almost lost while in WT their occupancy was still 7% (fig 4B). The actin cytoskeleton of *pi4kß1ß2* mutants thus appear to be more sensitive to latB. Meanwhile, we wanted to evaluate the impact of latB directly on the PI4P content using genetically encoded biosensor mCitrine-2xFAPP1 for PI4P (Simon et al., 2014). The sensor mostly labels PI4P localized in plasma membrane. In our setup, the content of PI4P remained stable in response to latB (fig.S3 A, C).

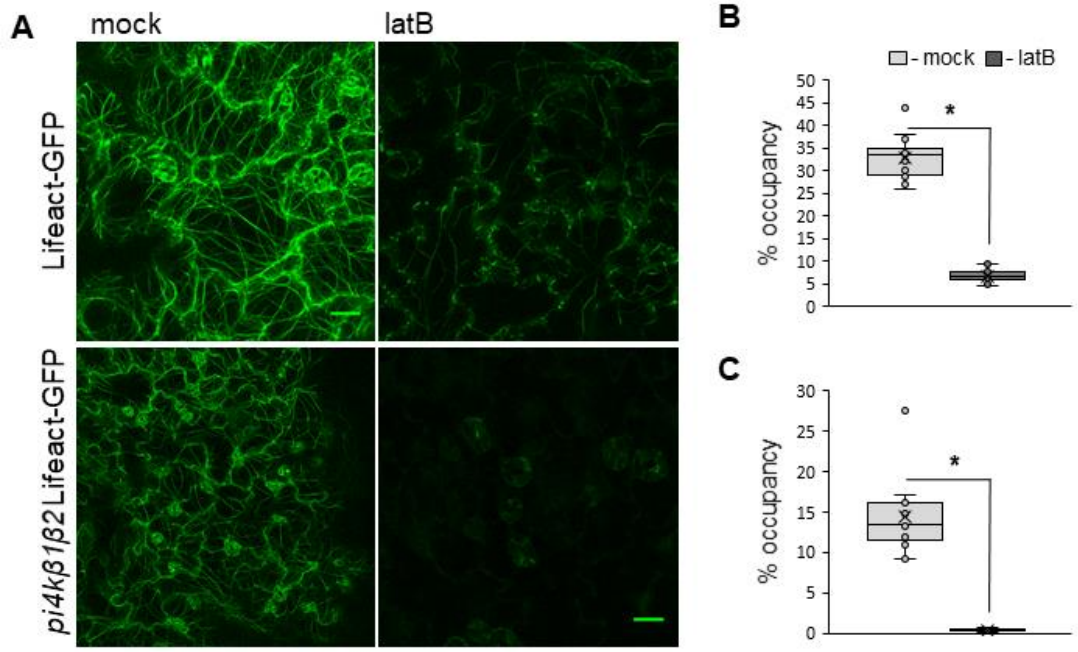

Figure 4. Effect of latB on actin filaments organization of *pi4kß1ß2* mutants. A. Representative images of maximum intensity projections of 10µm abaxial epidermis of LifeAct-GFP expressing WT and *pi4kß1ß2* plants. Confocal microscopy, scale bar = 20µm. Quantification of relative area occupied with fluorescent filament in WT (B) and *pi4kß1ß2* (C). For each variant at least 15 independent seedlings were imaged, n=12. For quantification, maximµm intensity projections of 10µm Z-stacks of abaxial sides of the leaves were used. At least 30 regions of interest (ROI) measured for each treatment. In the plots, central line represents the median occupancy, cross represents the mean, bottom and top edges of the box are 25 and 75% of distribution and the ends of whiskers are set at 1.5 times the interquartile range. Values outside this range are shown as outliers. Asterisks indicate statistically significant differences with the mock treatment, Student *t*-test, $p<0,05$

Effects of latB on callose accumulation in pi4kß1ß2 double mutant is still SA-independent

Because it seems there was a positive (enhancing) interaction between latB and PI4Kbeta mutations on actin filaments, we studied SA levels, callose accumulation and gene expression responses to latB in *pi4kß1ß2* plants. Indeed, latB triggered SA increase in *pi4kß1ß2* plants (fig. 5A). Surprisingly, introduction of neither *NahG* construct nor *pad4* mutation into *pi4kß1ß2* background did not fully prevent SA increase as it did in WT background (fig.2A), even though such an increase was still much lower than in WT or *pi4kß1ß2*. However, *sid2* mutation was sufficient to block SA production in both WT and *pi4kß1ß2*, confirming that the entire SA pool induced by latB treatment is synthetized due to ICS1 activity in both backgrounds. As for callose, its basal levels in 8-, 10- and 14-day-old *pi4kß1ß2* seedlings were similar to that of WT (Supplemental figure S4). To study the involvement of SA, the callose accumulation was also tested in triple mutants *NahGpi4kß1ß2* (Šašek et al, 2014), *sid2pi4kß1ß2* (Kalachova et al, 2019) and *pad4pi4kß1ß2*, obtained by crossing *pi4kß1ß2* to *pad4* (homozygous F3 plants were used). After latB treatment, accumulation of callose in all studied mutants was similar to that in WT (fig. 5B), suggesting that callose response to latB in *pi4kß1ß2* is still not SA-dependent (fig. 5B). This is consistent with our findings in WT plants.

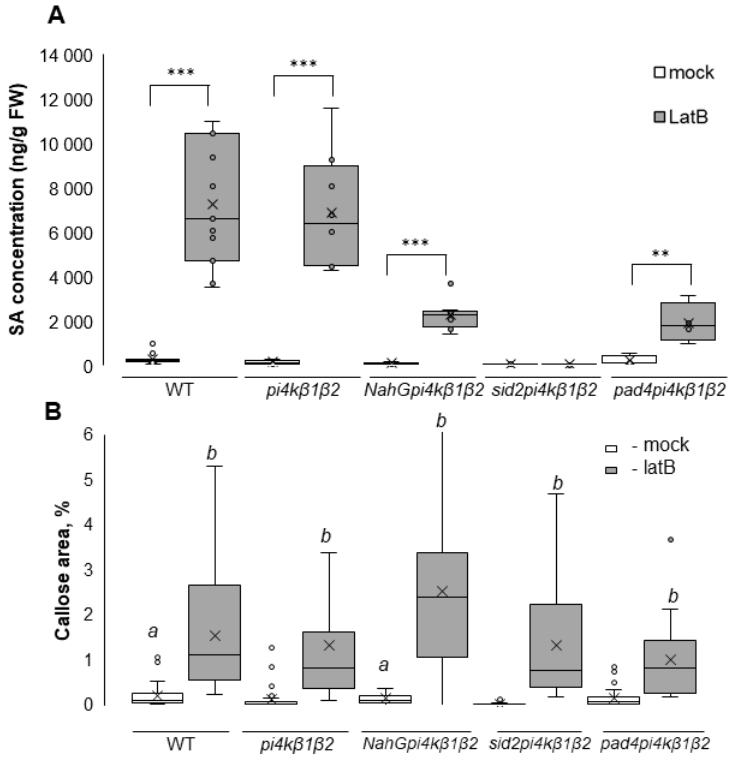

Figure 5. LatB induced SA and callose accumulation in *pi4kß1ß2* mutants. Ten-days-old seedlings were treated by 200 nM latB or 0.01% DMSO as mock control. Seedlings were harvested 24 hr after the treatment. A. SA content. Data from two independent experiments are plotted. B. Relative area of callose particles in the cotyledons. At least 30 independent cotyledons were analysed for each variant. Experiment was repeated three times with similar results, the data from a representative repetition are shown. In boxplots, central line represents the median occupancy, cross represents the mean, bottom and top edges of the box are 25 and 75% of distribution and the ends of whiskers are set at 1.5 times the interquartile range. Values outside this range are shown as outliers. Different letters mark significantly different values, p<0,05; Student *t*-test, unequal variance.

Effects of latrunculin B on defence genes expression in *pi4kß1ß2* double mutant

As for *PR1* and *WRKY38*, after latB treatment, their induction in *pi4kß1ß2* was comparable to that in WT. Yet, contrary to what was observed in WT background, their induction was also observed in *NahGpi4kß1ß2* and *pad4pi4kß1ß2* triple mutants (fig. 6). This is in agreement with the fact that SA is still accumulated in these triple mutants. *BAP1* expression in PI4K deficient mutants after latB treatment was induced less than in WT and was partly SA-dependent (fig. 6). Besides, neither induction of SA biosynthetic enzymes other than *ICS1* was detected, nor of JA-, ABA-, or ethylene markers (Supplemental figure S5, supplemental table ST2).

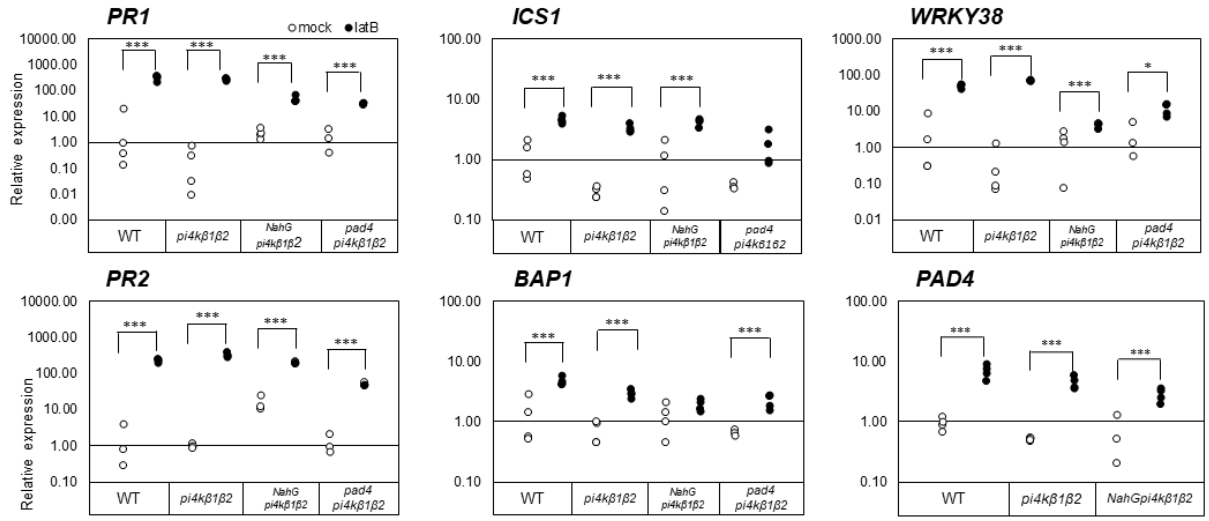

Figure 6. LatB–induced gene expression in *pi4kß1ß2* mutants. Ten-days-old seedlings of WT, *pi4kß1ß2, NahGpi4kß1ß2* and *pad4pi4kß1ß2* were treated by 200 nM latB or 0.01% DMSO as mock control. Seedlings were harvested 24 hr after the treatment. Data are normalized to mock-treated WT, note that data are plotted at the $\log_{10}$ scale. Asterisks indicate values, different from

respective controls for each genotype, * - p<0,05; *** - p<0.001, two-tailed Student *t*-test). Reference gene *TIP41*.

DISCUSSION

We show here that latrunculin B induces callose accumulation in seedlings. It is also true for cytochalasin E, another actin filament disruptor (data not shown). Therefore, it is very likely that this effect of latB is due to actin depolymerization. Callose deposition was reported in responses to various stresses, like wounding or pathogen infection (Jacobs et al, 2003). We had previously shown that chemical disruption of actin led to some immunity-related responses such as activation of *PR1* expression (Matouskova et al., 2014). In this regard, callose is particularly important, as another biotic-stress-like response, partly connected with SA. Arabidopsis genome encodes twelve callose synthases (Voigt, 2014). PMR4 (POWLDERY MILDEW RESISTANT 4, also called GLUCAN SYNTHASE LIKE 5, GLS5 or CALS12) is precisely the one activated during infection (Nishimura et al, 2003). Here we first show that callose accumulation induced by latB fully relies on PMR4. It indicates its connection with a biotic stress. Interestingly, using *NahG* and *pad4* mutants, we show that latrunculin B effects on callose accumulation is SA-independent and not downstream of PAD4. To be noted, *pmr4* mutant itself was reported to have a constitutively activated SA pathway in adult plants and contribute to most of callose accumulations in studies connected with biotics stres (Nishimura et al., 2003). Nevertheless, SA level in *pmr4* seedlings did not differ from that in WT (Supplementary table ST3). It was also true for *pi4kß1ß2* plants, known as SA and callose accumulators while being grown up to 4-weeks (Kalachova et al, 2019). However, neither SA nor callose levels were increased in non-stimulated seedlings (figure 5). A negative interaction between actin polymerisation, callose and SA levels has been suggested recently: natural polymorphism of genetic disruption of Actin Related Protein Complex 4 (ARPC4) affected pathogen- and wounding-induced callose deposition, as well as affected expression of *PR1* in response to *Sclerotinia sclerotiorum* (Badet et al, 2019).

As latB action on callose appeared as SA-independent, we wanted to check whether the effect of latB on gene expression was also independent on SA. We first better detailed the changes in gene expression triggered by latB. We show here that *PR1, PR2, WRKY38, ICS1* and *PAD4* were induced by latB in WT. It is also the case for a marker of cell death in pathogen and wounding responses, *BAP1* (Yang et al, 2007). *BAP1* was described as wounding marker, but also as a SA-

associated gene: it negatively regulates cell death in response to *Pseudomonas syringae* pv *tomato* and *Hyaloperonospora parasitica* acting in the same pathway with *BON1*, *SNC1* and *PAD4* (Yang et al, 2006) *BAP1* expression can be induced by high temperature or ROS formation, however this induction was abolished in mutants with altered SA pathways (*NahG, pad4*) (Hedtmann et al, 2017; Zhu et al, 2011). In our setup, the expression of BAP1 was increased independently of the SA content in plants, indicating a new role of this gene in plant stress responses. Yet, no significant changes were observed in the expression of SA biosynthetic genes other than ICS1 (*ICS2*, *PAL1*, *PAL2*, *PAL3*), nor in the expression of *LOX2* and *AOS*, a JA-biosynthesis marker genes, nor to the jasmonate responsive genes *VSP2* and *PDF1.2*. Genes involved in ethylene biosynthesis (*ACS2*) (Denoux et al, 2008), ethylene response (*ERF1, LEA4-1*)(Lorenzo et al, 2003) or to the response of abscisic acid (*ABI1*)(Leung et al, 1997) were not induced by latB. Therefore, it seems that latB action is not "universal", that it does not lead to a deregulation of the whole transcriptome. Its action seems to be directed mainly towards the SA signalling pathway or toward response to biotrophic pathogens.

Clearly, a SA dependent pathway is activated by latB. Expression of *PR1*, a classical representative of defence genes, is usually induced during pathogen attack, but also as a reaction to any SA increase. Besides, *ICS1*, that is responsible for most of the SA accumulation in response to bacteria (Li et al, 2019; Wildermuth et al, 2001; Zheng et al, 2015), was strongly induced. Therefore, the question was the following: did the changes in gene expression, that target SA responsive genes, occur through a SA-dependent pathway. We could show that the expression of *PR1* and *WRKY38* by latB relied on SA accumulation and a functional PAD4 protein. The fact that *ICS1* expression is controlled by PAD4 in response to pathogen was established (Cui et al., 2017). Yet, the expression of *PR2* and *ICS1* is independent on SA, as seen in the *NahGpi4kß1ß2*. *PR2* is one of the early defence genes, usually co-expressed with *PR1* and *PR5* and used as a marker of SA pathway (Hamamouch et al, 2011). Nevertheless, here we describe its clear SA-independent induction. It might seem contradictory, unless we take into account that PR2 protein is β-1,3-glucanase, particularly important for antifungal defences (Ali et al, 2018). PR2 is crucial for callose degradation and contributes to the SA increase; its overexpression enhances resistance both to fungal and bacterial pathogens (Oide et al, 2013).

It thus appears that latB (likely through its action on actin filaments) activates a signaling pathway typical of the response to pathogens. It activates PAD4. Some of the PAD4 action leads to *ICS1* expression, to SA accumulation and to the expression of SA responsive genes. Yet, a part of PAD4 action is not dependent on SA, as seen by *ICS1* expression. LatB also triggers a pathway that does not involve PAD4 nor SA, and that leads to callose accumulation and *PR2* expression.

The action of latB is likely to occur through actin filament depolymerization. Actin filaments are involved in the control of vesicle trafficking. Phosphoinositides are also involved in vesicular trafficking. There is indeed an interaction/interplay between actin filaments and phosphoinositides (Pleskot et al, 2014). F-actin capping protein interaction with actin monomers is regulated by phosphatidic acid and phosphatidylinositol-4,5-bisphosphate, a phosphoinositide (Pleskot et al, 2012). In pollen tube, cytoskeletal disruption by latB or jasplakinolide not only affects actin and arrested tube growth, but also causes relocalization and even dissociation of RabA4a and RabA4b-tagged vesicles (Zhang et al, 2010). Interestingly, PI4Kβ1 and PI4Kβ2 were shown to be recruited by RabA4b. Due to this interaction between actin and phosphoinositides in relation to vesicle trafficking, we were interested to investigate whether the action of latB could be impacted by alteration in phosphoinositide metabolism. To address this, *pi4kß1ß2* mutant was a tool of choice. As already mentioned, PI4Ks are the first enzymes that commit PI toward the synthesis of phosphoinositides, and the beta isoforms PI4Kβ1 and PI4Kβ2 were shown to be recruited by RabA4b. PI4Kbeta proteins participate in cytokinesis in Arabidopsis roots by targeting actin filaments to the cell plate (Lin et al, 2019). Nevertheless, it is important to consider the fact that *pi4kß1ß2* plants exhibit constitutive activation of SA-related genes and high basal levels of callose. Yet it is true for mature 4 week-old soil-grown plants (Antignani et al, 2015; Kalachova et al, 2019; Šašek et al, 2014). In younger plants, no *PR1* overexpression was detected (Sasek et al., 2014). In the present study we used 10-day-old seedlings grown *in vitro*. In these conditions, neither SA accumulation (fig.5 A, Supplementary table ST3), nor constitutively high expression of *PR1* and *ICS1* was observed (fig. 6).

The actin cytoskeleton of *pi4kß1ß2* mutants appear to be more sensitive to latB (fig.4). This is consistent with the above mentioned references which show F-actin capping protein interaction with actin monomers is regulated by phosphatidic acid and phosphatidylinositol-4,5-bisphosphate, a phosphoinositide (Pleskot et al, 2012). In response to latB, *pi4kß1ß2* seedlings

accumulated callose, in a SA- and PAD4- independent way, as observed in WT plants. Yet, when we assay the SA increase in response to latB, a process not observed in WT is then detected: the SA induction in *pi4kß1ß2* background still occurs, despite the mutation in PAD4 or expression of NahG. The *pi4kß1ß2* double mutation allows to reveal a signalling pathway, triggered here by latB, that leads to SA biosynthesis and *PR1* expression independently on PAD4. Yet, the *PR1* expression in response to latB was not only observed in *NahGpi4kß1ß2* and *pad4pi4kß1ß2* triple mutants, but also in *sid2pi4kß1ß2* (data not shown). Therefore, our data on the existence of such a SA independent pathway are strong. Is this pathway usually actively inhibited by functional PI4Ks? Is it linked to the effect of *pi4kß1ß2* double mutation on trafficking? Or is it due to a role of phosphoinositide on signalling? An important contribution may come from immune-related MAPKs, whose transient or sustained activation works as a switch between pattern-triggered immunity and effector triggered immunity (Tsuda et al, 2013). Indeed, *Tsuda et al.* described expression of *PR1* in *sid2* background, induced by constitutive activation of MPK3 and MPK6. Another enzyme of the cascade, MPK4, was shown to interact with PI4Kβ1 during cell plate formation in cytokinesis (Lin et al, 2019). More research is necessary to understand and characterize this pathway.

To summarize, we here report the defence-like consequences of actin cytoskeleton disruption by latB (fig. 7). Two kinds of signalling pathways were activated by latB treatment: a first pathway is independent on SA; it leads to the expression of genes such as *PR2*, but also to callose accumulation through PMR4. The second pathway involves SA synthesis via PAD4 and ICS1; it leads to the expression of genes such as *PR1* and *WRKY38*. The double mutation in PI4Kß1ß2 makes the effect of latB on filaments more pronounced. Interestingly, the SA increase and *PR1* expression in response to latB in the *pi4kß1ß2* background is also triggered in an unconventional, PAD4-independent pathway. Either this pathway is actively inhibited in WT background by PI4Kß1ß2 (and thus not seen), or it is activated only when the PI4Kß1ß2 are missing.

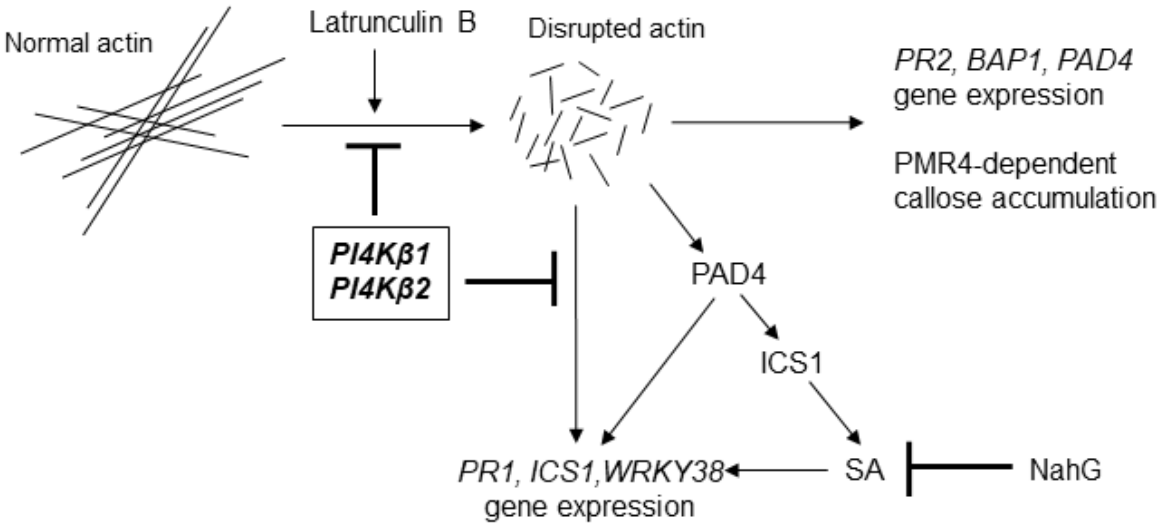

Figure 7. **Graphical summary of the latrunculin B effects in seedlings**. The disruption of actin polymers by latB activates two kinds of signalling pathways. A first pathway is independent on SA; it leads to the expression of genes such as *PR2*, but also to callose accumulation. The second pathway involves SA synthesis via PAD4 and ICS1; it leads to the expression of genes such as *PR1* and *WRKY38*. The double mutation in PI4K beta1 and beta2 makes the effect of latB on filaments more pronounced. Interestingly, the *PR1* expression in response to latB is no longer SA-dependent in the *pi4kß1ß2* background: a SA independent pathway leading to *PR1* expression is thus revealed.

Still several open questions remain: what makes actin depolymerization trigger these pathways? Is it the disrupted actin *per se* that act? Or are these pathways activated as a response to a process altered due to lack of good filaments? Such a process could be a modified vesicle trafficking due the missing actin filaments. In this regard, it would be interesting to monitor the processing of receptors of MAMPs in seedlings submitted to artificial cytoskeleton depolymerization agents.

We believe this work sheds light on the connection between cytoskeleton dynamics, vesicular trafficking and immunity at the cellular and subcellular level and thus will contribute to better understanding of plant responses to changing environment.

FUNDING INFORMATION

This work was supported by Czech Science Foundation [GAČR grant no. 17-05151S]. TK benefited from the Program of Postdoctoral Fellowships of the Czech Academy of Sciences [PPPLZ grant no. TK 919220]. OI received the Visegrad scholarship (2018–2019) [grant no. 51810647]. HL benefited from Charles University student grant [GAUK no. 992416]. The work was also supported by the Ministry of Education, Youth and Sports of CR from European Regional Development Fund-Project "Centre for Experimental Plant Biology" [grant no. CZ.02.1.01/0.0/0.0/16_019/0000738]. IEB imaging facility is supported by OPPK CZ.2.16/3.1.00/21519.

ACKNOWLEDGEMENTS

We are very grateful to Dr. Ivan Kulich for providing pUBQ::PMR4-GFP expressing lines and Dr. Yvon Jaillais for mCitrine-2xFAPP1 expressing line. We would like to thank Dr. Kateřina Malínská for training and the precious advices with microscopy.

AUTHOR CONTRIBUTION

TK, MJ and ER - conceptualization; TK, OI, HL, PM, PK and RP - data curation; TK, HL, OI - formal analysis; TK, HL, OI, DK, PM - methodology; LB, OV, JM - funding acquisition, resources, project administration; TK, HL – writing, original draft; TK, MJ, LB, ER - review & editing. All authors commented and approved the manuscript. Authors declare no conflict of interests.

SUPPLEMENTARY DATA:

Supplemental figure S1. LatB treatment did not cause cell death in seedlings. A. Actin depolymerization after latB treatment. Representative confocal images of abaxial epidermis of 10-days-old *A.thaliana* seedlings expressing Lifeact-GFP treated with for 24h with 0.05% DMSO (mock) of 200nM latB. Confocal microscopy, scale bar = 20µm. B. Trypan blue staining of seedlings. Boiling for 5min was used as a positive control for cell death; color camera, scale bar = 500µm.

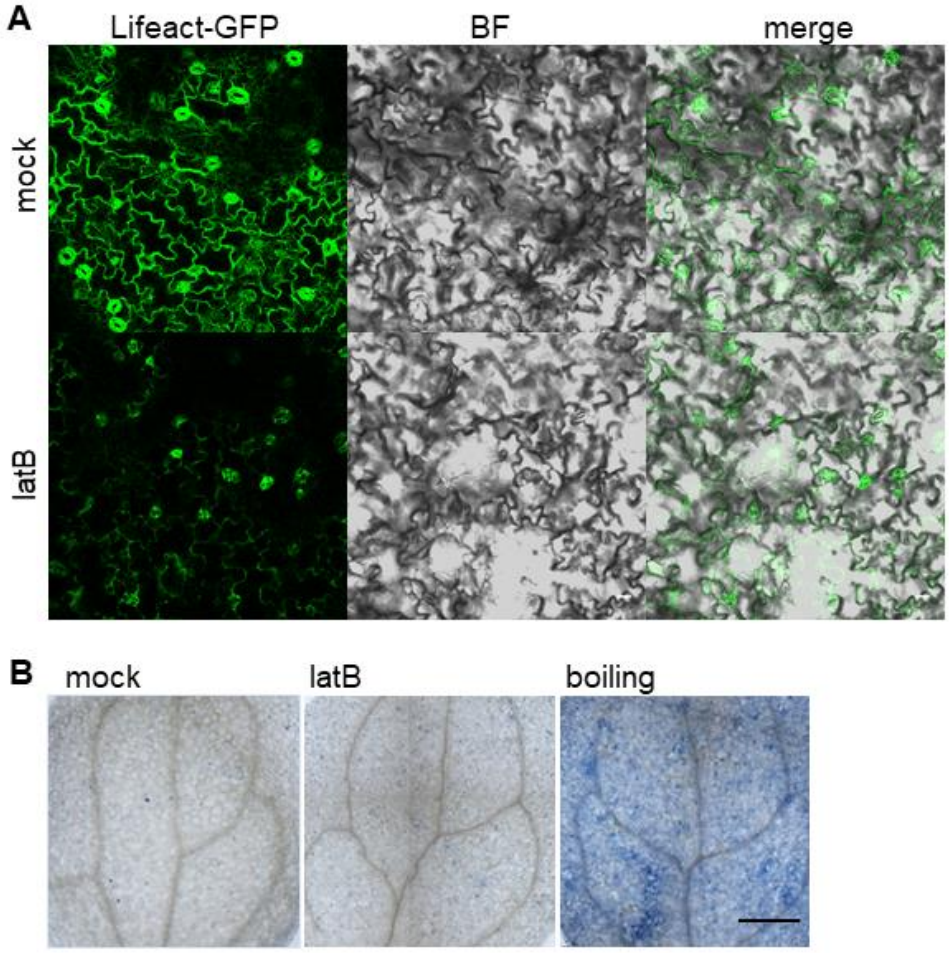

Supplementary figure S2. Relative expression of SA biosynthesis and JA marker genes in *NahG* and *pad4* mutants. Ten-days-old seedlings of WT, *NahG* and *pad4* were treated by 200 nM latB or 0.01% DMSO as mock control. Seedlings were harvested 24 hr after the treatment. Data are normalized to mock-treated WT, note that data are plotted at the $\log_{10}$ scale. Asterisks indicate values, different from respective controls for each genotype, * - p<0,05; *** - p<0.001, two-tailed Student *t*-test). Reference gene *TIP41*.

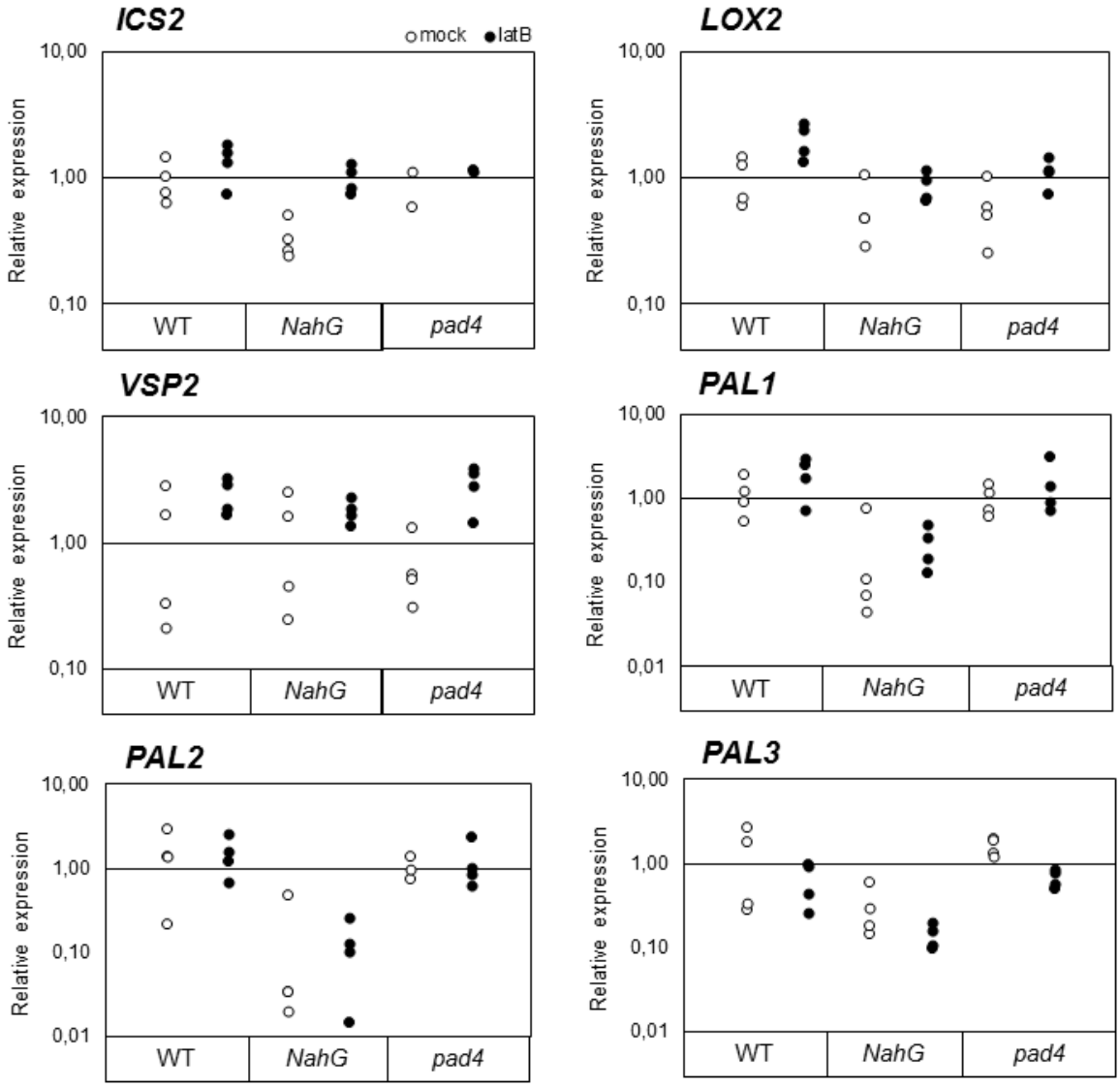

Supplemental figure S3. LatB decrease actin filaments abundance while PI4P level remains stable. Ten-days-old seedlings were imaged 24h after replacing cultivation media with 0.05% DMSO (Mock) of 200nM latrunculin B (latB). For each variant at least 10 individual seedlings were observed. A. Representative images of the cotyledons of Lifeact-GFP and mCitrine-2xFAPP1 expressing plants after latB treatment; confocal microscopy, scale bar 20µm. Quantification of the actin filaments by lifeact-GFP signal intensity (B); PI4P levels by mCitrine-2xFAPP1 fluorescent signal intensity (C). For quantification, maximum intensity projections of 10µm Z-stacks of abaxial sides of the leaves were used. At least 30 regions of interest (ROI) measured for each treatment. In the plots, central line represents the median occupancy, cross represents the mean, bottom and top edges of the box are 25 and 75% of distribution and the ends of whiskers are set at 1.5 times the interquartile range. Values outside this range are shown as outliers. Asterisks indicate statistically significant differences with the mock treatment, Student *t*-test, $p<0,05$

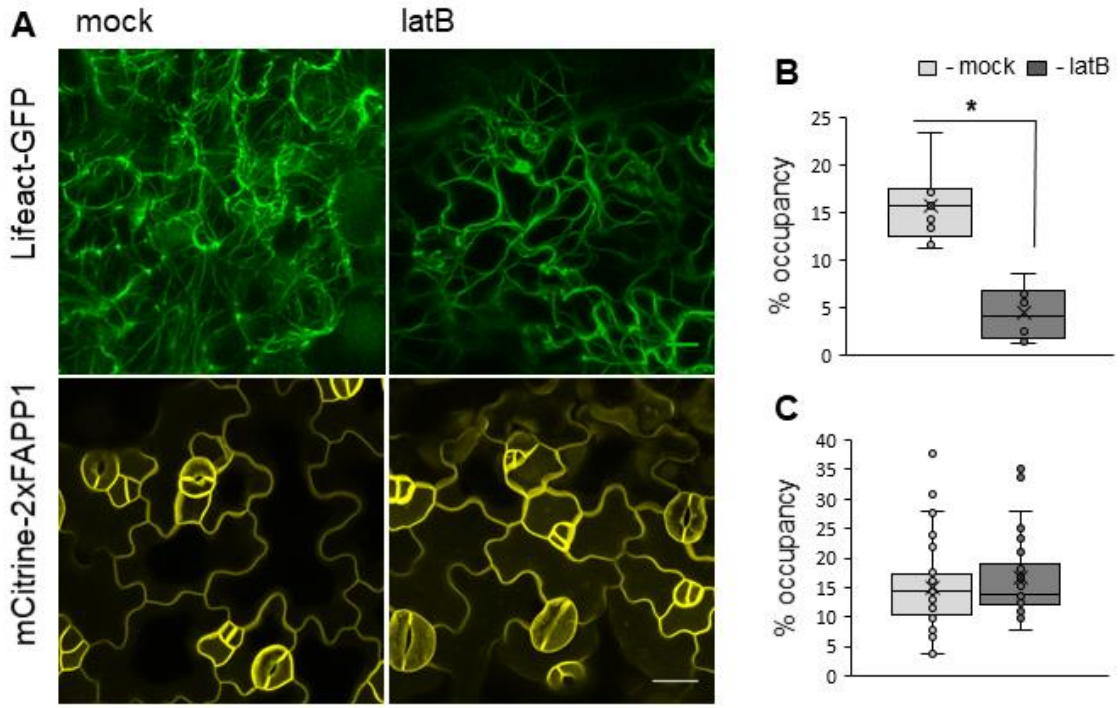

Supplemental figure S4. Representative images of basal callose accumulation in WT and *pi4kß1ß2* seedlings. Anilin blue staining, epifluorescent microscopy, scale bar 500µm.

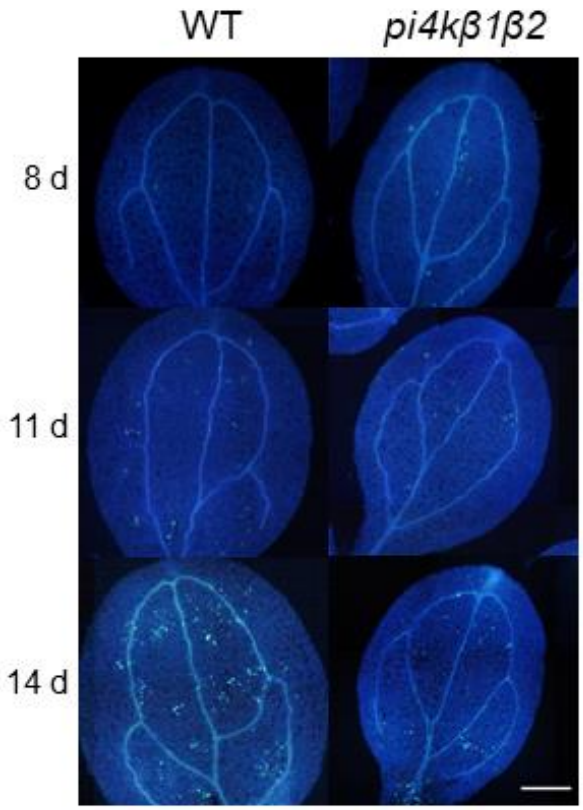

Supplementary figure S5. Relative expression of SA biosynthesis and JA marker genes in *pi4kß1ß2* mutants. Ten-days-old seedlings of WT, *pi4kß1ß2*, *NahGpi4kß1ß2* and *pad4pi4kß1ß2* were treated by 200 nM latB or 0.01% DMSO as mock control. Seedlings were harvested 24 h after the treatment. Data are normalized to mock-treated WT, note that data are plotted at the $\log_{10}$ scale. Asterisks indicate values, different from respective controls for each genotype, * - p<0,05; *** - p<0.001, two-tailed Student *t*-test). Reference gene *TIP41*.

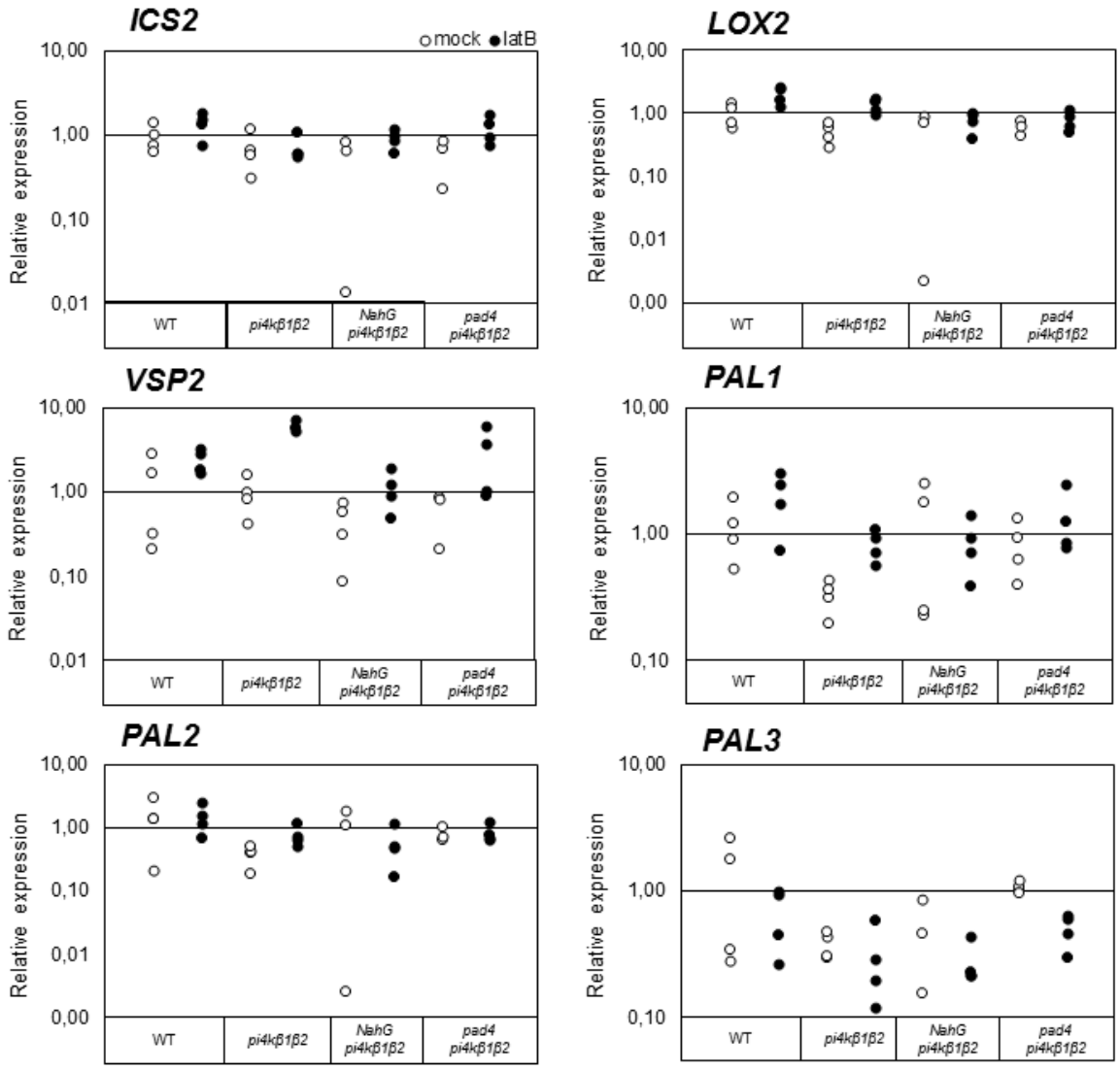

Supplemental table ST1. Primers used in this study

Gene	Accession number	Forward primer	Reverse primer
TIP41	AT4G34270	GTGAAAACTGTTGGAGAGAAGCAA	TCAACTGGATACCCTTTCGCA
PR1	AT2G14610	AGTTGTTTGGAGAAAGTCAG	GTTCACATAATTCCCACGA
PR2	AT3G57260	TATAGC CAC TGA CAC CAC	GCCAAGAAACCTATCACTG
ICS1	At1g74710	GCAAGAATCATGTTCCTACC	AATTATCCTGCTGTTACGAG
ICS2	AT1G18870	TGTCTTCAAAGTCTCCTCTG	CTTCCTCCAAACTCATCAAAC
WRKY38	At5g22570	GCCCCTCCAAGAAAAGAAAG	CCTCCAAAGATACCCGTCGT
LOX2	AT3G45140	ATCCCACCTCACTCATTACT	ATCCAACACGAACAATCTCT
VSP2	AT5G24770	CCAAACAGTACCAATACGAC	CTTCTCTGTTCCGTATCCAT
PAL1	AT2G37040	GTGTCGCACTTCAGAAGGAA	GGCTTGTTTCTTTCGTGCTT
PAL2	AT3G53260	GTGCTACTTCTCACCGGAGA	TATTCCGGCGTTCAAAAATC
PAL3	AT5G04230	CAACCAAACGCAACAGCA	CTCCAGGTGGCTCCCTTTTA
PAD4	AT3G52430	GGTTCTGTTCGTCTGATGTT	GTTCCTCGGTGTTTTGAGTT
BAP1	At3g61190	ATGCCCATCAATGGTAATG	TCCCACACTTATCACCAAA
PDF1.2a	AT5G44420	ACGCACCGGCAATGGTGGAA	TGCATGATCCATGTTTGGCT
PDF1.2c	AT5G44430	CTGCTACCATCATCACCTTC	CCGCAAACGCCTGACCATGT
AOS	AT5G42650	GGTCATCAAGTTCATAACCG	TTTCTCAATCGCTCCCAT
ACS2	At1g01480	GTTAAGCTCAATGTGTCTCC	AAGCAAATCCTAAACCATCC
ERF1	At3g23240	ATCAAATCCGTAAGCTCAAG	CCAAACCCTAATACCGTTTC
LEA4-1	AT1G32560	AGCAAAAGCTGATGAGAAGGCA	TAGGTCTGAGGAGGCACTGA
ABI1	AT4G26080	ATGTCGAGATCCATTGGCGAT	TTCCTTTCTCCGCTCATCCG
PMR4	AT4G03550	ATGTACACATGTAAATGGCG	GAGGCTGGGTCTCGAGGAGTT

Supplemental table ST2. Effect of latB on defence gene expression.

	WT		*NahG*		*pad4*		*pi4kβ1β2*		*NahGpi4kβ1β2*		*pad4pi4kβ1β2*	
	mock	LatB	mock	LatB	mock	LatB	mock	LatB	mock	LatB	mock	LatB
PdF1.2a	1.03 ± 0.29	3.48 ± 0.64	2.22 ± 0.78	2.25 ± 0.32	1.84 ± 0.21	4.50 ± 0.70	1.72 ± 0.18	4.79 ± 0.92	3.49 ± 0.54	13.29 ± 2.34	4.67 ± 0.67	4.91 ± 0.96
PdF1.2c	1.17 ± 0.43	4.64 ± 1.05	1.82 ± 0.66	2.78 ± 0.37	2.15 ± 0.31	6.00 ± 1.05	1.73 ± 0.20	6.93 ± 1.55	2.34 ± 0.34	16.99 ± 5.05	4.15 ± 0.69	5.75 ± 1.25
ACS2	3.83 ± 2.15	2.20 ± 0.16	3.07 ± 0.33	4.97 ± 1.12	8.81 ± 1.30	42.83 ± 7.80	0.47 ± 0.18	2.13 ± 0.21	5.05 ± 0.87	10.43 ± 1.26	1.40 ± 0.12	10.30 ± 3.72
AOS	1.14 ± 0.39	6.07 ± 0.87	0.48 ± 0.15	1.27 ± 0.44	1.26 ± 0.67	2.05 ± 1.24	0.62 ± 0.14	2.15 ± 0.28	1.60 ± 0.76	5.08 ± 1.14	2.69 ± 0.92	5.82 ± 1.63
ERF1	2.05 ± 0.80	8.57 ± 0.55	1.09 ± 0.12	5.82 ± 0.55	2.86 ± 0.33	13.32 ± 1.90	0.82 ± 0.27	5.99 ± 0.68	2.51 ± 0.80	13.83 ± 0.92	3.13 ± 0.23	11.10 ± 1.91
LEA4-1	1.14 ± 0.32	1.35 ± 0.23	1.21 ± 0.24	0.87 ± 0.24	0.82 ± 0.15	1.29 ± 0.19	0.93 ± 0.12	0.97 ± 0.07	0.95 ± 0.22	1.25 ± 0.29	3.45 ± 2.07	0.92 ± 0.13
ABI1	0.98 ± 0.04	1.18 ± 0.03	0.89 ± 0.05	1.13 ± 0.06	0.00 ± 0.00	0.00 ± 0.00	0.56 ± 0.02	0.79 ± 0.03	0.00 ± 0.00	0.00 ± 0.00	0.00 ± 0.00	0.00 ± 0.00

Supplemental table ST3. Effect of latB on salicylic acid content in seedlings. Seedlings were grown *in vitro* for 10 days and treated with 1µM latB for 24h. DMSO was used as mock treatment. SA content was measured by LC-MS. Means ± SE from 8 values generated in two independent experiments are shown.

SA content (ng/ g FW)	DMSO			LatB		
WT	307,70	±	66,59	7247,39	±	793,85
pmr4	402,10	±	45,02	10179,89	±	756,35
NahG	64,11	±	6,30	451,38	±	51,03
sid2	54,30	±	6,84	54,84	±	3,32
pad4	102,97	±	20,15	788,84	±	158,57
pi4kβ1β2	159,56	±	26,04	6879,74	±	864,17
NahGpi4kβ1β2	105,50	±	18,14	2286,92	±	222,89
sid2pi4kβ1β2	60,94	±	9,76	62,75	±	10,80
pad4pi4kβ1β2	237,77	±	92,15	1925,06	±	385,01

REFERENCES

1. Ali S, Ganai BA, Kamili AN, Bhat AA, Mir ZA, Bhat JA, Tyagi A, Islam ST, Mushtaq M, Yadav P, Rawat S, Grover A (2018) Pathogenesis-related proteins and peptides as promising tools for engineering plants with multiple stress tolerance. *Microbiol Res* **212-213:** 29-37

2. Andreeva Z, Barton D, Armour W, Li M, Liao L-F, McKellar H, Pethybridge K, Marc J (2010) Inhibition of phospholipase C disrupts cytoskeletal organization and gravitropic growth in <i>Arabidopsis</i> roots. *Planta* **232:** 1263-1279

3. Antignani V, Klocko AL, Bak G, Chandrasekaran SD, Dunivin T, Nielsen E (2015) Recruitment of PLANT U-BOX13 and the PI4Kβ1/β2 Phosphatidylinositol-4 Kinases by the Small GTPase RabA4B Plays Important Roles during Salicylic Acid-Mediated Plant Defense Signaling in Arabidopsis. *The Plant Cell* **27:** 243-261

4. Badet T, Léger O, Barascud M, Voisin D, Sadon P, Vincent R, Le Ru A, Balagué C, Roby D, Raffaele S (2019) Expression polymorphism at the ARPC4 locus links the actin cytoskeleton with quantitative disease resistance to Sclerotinia sclerotiorum in Arabidopsis thaliana. *New Phytol* **222:** 480-496

5. Baluška F, Jasik J, Edelmann HG, Salajová T, Volkmann D (2001) Latrunculin B-Induced Plant Dwarfism: Plant Cell Elongation Is F-Actin-Dependent. *Dev Biol* **231:** 113-124

6. Bigeard J, Colcombet J, Hirt H (2015) Signaling Mechanisms in Pattern-Triggered Immunity (PTI). *Mol Plant* **8:** 521-539

7. Brill JA, Hime GR, Scharer-Schuksz M, Fuller MT (2000) A phospholipid kinase regulates actin organization and intercellular bridge formation during germline cytokinesis. *Development* **127:** 3855-3864

8. Chen X-Y, Kim J-Y (2009) Callose synthesis in higher plants. *Plant Signaling Behav* **4:** 489-492

9. Chen X-Y, Liu L, Lee E, Han X, Rim Y, Chu H, Kim S-W, Sack F, Kim J-Y (2009) The Arabidopsis callose synthase gene GSL8 is required for cytokinesis and cell patterning. *Plant Physiol* **150:** 105-113

10. Cui H, Gobbato E, Kracher B, Qiu J, Bautor J, Parker JE (2017) A core function of EDS1 with PAD4 is to protect the salicylic acid defense sector in Arabidopsis immunity. *New Phytol* **213:** 1802-1817

11. Cui W, Lee J-Y (2016) Arabidopsis callose synthases CalS1/8 regulate plasmodesmal permeability during stress. *Nature Plants* **2:** 16034

12. Cvrčková F, Oulehlová D (2017) A new kymogram-based method reveals unexpected effects of marker protein expression and spatial anisotropy of cytoskeletal dynamics in plant cell cortex. *Plant Methods* **13:** 19

13. Delage E, Puyaubert J, Zachowski A, Ruelland E (2013) Signal transduction pathways involving phosphatidylinositol 4-phosphate and phosphatidylinositol 4,5-bisphosphate: Convergences and divergences among eukaryotic kingdoms. *Prog Lipid Res* **52:** 1-14

14. Delaney T, Uknes S, Vernooij B, Friedrich L, Weymann K, Negrotto D, Gaffney T, Gut-Rella M, Kessmann H, Ward E, Ryals J (1994) A central role of salicylic acid in plant disease resistance. *Science* **266:** 1247 - 1250

15. Denoux C, Galletti R, Mammarella N, Gopalan S, Werck D, De Lorenzo G, Ferrari S, Ausubel FM, Dewdney J (2008) Activation of defense response pathways by OGs and Flg22 elicitors in Arabidopsis seedlings. *Mol Plant* **1:** 423-445

16. Drobak BK, Franklin-Tong VE, Staiger CJ (2004) The Role of the Actin Cytoskeleton in Plant Cell Signaling. *The New Phytologist* **163:** 13-30

17. Ebine K, Ueda T (2015) Roles of membrane trafficking in plant cell wall dynamics. *Front Plant Sci* **6**

18. Ellinger D, Glöckner A, Koch J, Naumann M, Stürtz V, Schütt K, Manisseri C, Somerville SC, Voigt CA (2014) Interaction of the Arabidopsis GTPase RabA4c with Its Effector PMR4 Results in Complete Penetration Resistance to Powdery Mildew. *The Plant Cell* **26:** 3185-3200

19. Fernández-Bautista N, Domínguez-Núñez JA, Moreno MMC, Berrocal-Lobo M (2016) Plant Tissue Trypan Blue Staining During Phytopathogen Infection. *Bio-protocol* **6:** e2078

20. Geitmann A, Nebenführ A (2015) Navigating the plant cell: intracellular transport logistics in the green kingdom. *Mol Biol Cell* **26:** 3373-3378

21. Gibbon BC, Kovar DR, Staiger CJ (1999) Latrunculin B has different effects on pollen germination and tube growth. *The Plant cell* **11:** 2349-2363

22. Hamamouch N, Li C, Seo PJ, Park C-M, Davis EL (2011) Expression of Arabidopsis pathogenesis-related genes during nematode infection. *Mol Plant Pathol* **12:** 355-364

23. Hardham AR (2007) Cell biology of plant–oomycete interactions. *Cell Microbiol* **9:** 31-39

24. Hedtmann C, Guo W, Reifschneider E, Heiber I, Hiltscher H, van Buer J, Barsch A, Niehaus K, Rowan B, Lortzing T, Steppuhn A, Baier M (2017) The Plant Immunity Regulating F-Box Protein CPR1 Supports Plastid Function in Absence of Pathogens. *Front Plant Sci* **8**

25. Henty-Ridilla JL, Shimono M, Li J, Chang JH, Day B, Staiger CJ (2013) The Plant Actin Cytoskeleton Responds to Signals from Microbe-Associated Molecular Patterns. *PLOS Pathogens* **9:** e1003290

26. Jacobs AK, Lipka V, Burton RA, Panstruga R, Strizhov N, Schulze-Lefert P, Fincher GB (2003) An Arabidopsis Callose Synthase, GSL5, Is Required for Wound and Papillary Callose Formation. *The Plant Cell* **15:** 2503-2513

27. Kalachova T, Janda M, Šašek V, Ortmannová J, Nováková P, Dobrev IP, Kravets V, Guivarc'h A, Moura D, Burketová L, Valentová O, Ruelland E (2019) Identification of salicylic acid-independent responses in an Arabidopsis phosphatidylinositol 4-kinase beta double mutant. *Annals of Botany*

28. Kang B-H, Nielsen E, Preuss ML, Mastronarde D, Staehelin LA (2011) Electron Tomography of RabA4b- and PI-4Kβ1-Labeled Trans Golgi Network Compartments in Arabidopsis. *Traffic* **12:** 313-329

29. Keppler BD, Song J, Nyman J, Voigt CA, Bent AF (2018) 3-Aminobenzamide Blocks MAMP-Induced Callose Deposition Independently of Its Poly(ADPribosyl)ation Inhibiting Activity. *Front Plant Sci* **9:** 1907-1907

30. Kulich I, Vojtíková Z, Sabol P, Ortmannová J, Neděla V, Tihlaříková E, Žárský V (2018) Exocyst Subunit EXO70H4 Has a Specific Role in Callose Synthase Secretion and Silica Accumulation. *Plant Physiol* **176:** 2040-2051

31. Leontovyčova H, Kalachova T, Trda L, Lamparova L, Pospichalova R, Dobrev P, Malinska K, Burketova L, Valentova O, Janda M (2019) Actin depolymerization is able to increase plant resistance against pathogens via activation of salicylic acid signalling pathway. *Scientific Reports* **in press**

32. Leung J, Merlot S, Giraudat J (1997) The Arabidopsis ABSCISIC ACID-INSENSITIVE2 (ABI2) and ABI1 genes encode homologous protein phosphatases 2C involved in abscisic acid signal transduction. *The Plant cell* **9:** 759-771

33. Li J, Cao L, Staiger CJ (2017) Capping Protein Modulates Actin Remodeling in Response to Reactive Oxygen Species during Plant Innate Immunity. *Plant Physiol* **173:** 1125-1136

34. Li N, Han X, Feng D, Yuan D, Huang L-J (2019) Signaling Crosstalk between Salicylic Acid and Ethylene/Jasmonate in Plant Defense: Do We Understand What They Are Whispering? *International Journal of Molecular Sciences* **20:** 671

35. Lin F, Krishnamoorthy P, Schubert V, Hause G, Heilmann M, Heilmann I (2019) A dual role for cell plate-associated PI4Kβ in endocytosis and phragmoplast dynamics during plant somatic cytokinesis. *The EMBO Journal* **38:** e100303

36. Lorenzo O, Piqueras R, Sánchez-Serrano JJ, Solano R (2003) ETHYLENE RESPONSE FACTOR1 integrates signals from ethylene and jasmonate pathways in plant defense. *The Plant cell* **15:** 165-178

37. Lu Y-J, Day B (2017) Quantitative Evaluation of Plant Actin Cytoskeletal Organization During Immune Signaling. *Methods in molecular biology (Clifton, NJ)* **1578:** 207-221

38. Matoušková J, Janda M, Fišer R, Šašek V, Kocourková D, Burketová L, Dušková J, Martinec J, Valentová O (2014) Changes in actin dynamics are involved in salicylic acid signaling pathway. *Plant Sci* **223:** 36-44

39. Morton WM, Ayscough KR, McLaughlin PJ (2000) Latrunculin alters the actin-monomer subunit interface to prevent polymerization. *Nat Cell Biol* **2:** 376

40. Moscatelli A, Idilli AI, Rodighiero S, Caccianiga M (2012) Inhibition of actin polymerisation by low concentration Latrunculin B affects endocytosis and alters exocytosis in shank and tip of tobacco pollen tubes. *Plant Biol* **14:** 770-782

41. Nishimura MT, Stein M, Hou B-H, Vogel JP, Edwards H, Somerville SC (2003) Loss of a Callose Synthase Results in Salicylic Acid-Dependent Disease Resistance. *Science* **301:** 969

42. Oide S, Bejai S, Staal J, Guan N, Kaliff M, Dixelius C (2013) A novel role of PR2 in abscisic acid (ABA) mediated, pathogen-induced callose deposition in Arabidopsis thaliana. *New Phytol* **200:** 1187-1199

43. Pleskot R, Pejchar P, Staiger CJ, Potocký M (2014) When fat is not bad: the regulation of actin dynamics by phospholipid signaling molecules. *Front Plant Sci* **5:** 5-5

44. Pleskot R, Pejchar P, Žárský V, Staiger CJ, Potocký M (2012) Structural Insights into the Inhibition of Actin-Capping Protein by Interactions with Phosphatidic Acid and Phosphatidylinositol (4,5)-Bisphosphate. *PLOS Computational Biology* **8:** e1002765

45. Šašek V, Janda M, Delage E, Puyaubert J, Guivarc'h A, López Maseda E, Dobrev PI, Caius J, Bóka K, Valentová O, Burketová L, Zachowski A, Ruelland E (2014) Constitutive salicylic acid accumulation in pi4kIIIβ1β2 Arabidopsis plants stunts rosette but not root growth. *New Phytol* **203:** 805-816

46. Sassmann S, Rodrigues C, Milne SW, Nenninger A, Allwood E, Littlejohn GR, Talbot NJ, Soeller C, Davies B, Hussey PJ, Deeks MJ (2018) An Immune-Responsive Cytoskeletal-Plasma Membrane Feedback Loop in Plants. *Current biology : CB* **28:** 2136-2144.e2137

47. Schindelin J, Arganda-Carreras I, Frise E, Kaynig V, Longair M, Pietzsch T, Preibisch S, Rueden C, Saalfeld S, Schmid B, Tinevez J-Y, White DJ, Hartenstein V, Eliceiri K, Tomancak P, Cardona A (2012) Fiji: an open-source platform for biological-image analysis. *Nat Meth* **9:** 676

48. Schneider R, Hanak T, Persson S, Voigt CA (2016) Cellulose and callose synthesis and organization in focus, what's new? *Curr Opin Plant Biol* **34:** 9-16

49. Shimono M, Lu Y-J, Porter K, Kvitko BH, Henty-Ridilla J, Creason A, He SY, Chang JH, Staiger CJ, Day B (2016) The Pseudomonas syringae Type III Effector HopG1 Induces Actin Remodeling to Promote Symptom Development and Susceptibility during Infection. *Plant Physiol* **171:** 2239-2255

50. Simon MLA, Platre MP, Assil S, van Wijk R, Chen WY, Chory J, Dreux M, Munnik T, Jaillais Y (2014) A multi-colour/multi-affinity marker set to visualize phosphoinositide dynamics in Arabidopsis. *Plant J* **77:** 322-337

51. Thiele K, Wanner G, Kindzierski V, Jürgens G, Mayer U, Pachl F, Assaad FF (2009) The timely deposition of callose is essential for cytokinesis in Arabidopsis. *Plant J* **58:** 13-26

52. Tsuda K, Mine A, Bethke G, Igarashi D, Botanga CJ, Tsuda Y, Glazebrook J, Sato M, Katagiri F (2013) Dual regulation of gene expression mediated by extended MAPK activation and salicylic acid contributes to robust innate immunity in Arabidopsis thaliana. *PLoS genetics* **9:** e1004015-e1004015

53. Voigt CA (2014) Callose-mediated resistance to pathogenic intruders in plant defense-related papillae. *Front Plant Sci* **5:** 168

54. Wildermuth MC, Dewdney J, Wu G, Ausubel FM (2001) Isochorismate synthase is required to synthesize salicylic acid for plant defence. *Nature* **414:** 562-565

55. Yang H, Li Y, Hua J (2006) The C2 domain protein BAP1 negatively regulates defense responses in Arabidopsis. *Plant J* **48:** 238-248

56. Yang H, Yang S, Li Y, Hua J (2007) The Arabidopsis BAP1 and BAP2 genes are general inhibitors of programmed cell death. *Plant Physiol* **145:** 135-146

57. Záveská Drábková L, Honys D (2017) Evolutionary history of callose synthases in terrestrial plants with emphasis on proteins involved in male gametophyte development. *PloS one* **12:** e0187331-e0187331

58. Zhang Y, He J, Lee D, McCormick S (2010) Interdependence of Endomembrane Trafficking and Actin Dynamics during Polarized Growth of Arabidopsis Pollen Tubes. *Plant Physiol* **152:** 2200-2210

59. Zheng X-y, Zhou M, Yoo H, Pruneda-Paz JL, Spivey NW, Kay SA, Dong X (2015) Spatial and temporal regulation of biosynthesis of the plant immune signal salicylic acid. *PNAS* **112:** 9166

60. Zhu Y, Yang H, Mang H-G, Hua J (2011) Induction of BAP1 by a moderate decrease in temperature is mediated by ICE1 in Arabidopsis. *Plant Physiol* **155:** 580-588